The Development of a Low Carbon Binder Produced from the Ternary Blending of Cement, Ground Granulated Blast Furnace Slag and High Calcium Fly Ash: An Experimental and Statistical Approach

Ali Abdulhussein Shubbar [a] *, Hassnen Jafer [b], Anmar Dulaimi [c], Khalid Hashim [d]

William Atherton [d], Monower Sadique [d]

[a] Department of Civil Engineering, Liverpool John Moores University, Henry Cotton Building, Webster Street, Liverpool L3 2ET, UK

[b] Department of Civil Engineering, College of Engineering, University of Babylon, Babylon, Iraq

[c] Department of Civil Engineering, College of Engineering, Warith AL-Anbiya'a University, Kerbala, Iraq

[d] Department of Civil Engineering, Liverpool John Moores University, Peter Jost Enterprise Centre, Byrom Street, Liverpool, L3 3AF, UK.

* Corresponding author:

E-mail address: alishubbar993@gmail.com, A.A.Shubbar@2014.ljmu.ac.uk (A. Shubbar)

Abstract

This research aims to develop a new, environmentally friendly, cementitious material by blending Ordinary Portland Cement (OPC), Ground Granulated Blast Furnace Slag (GGBS) and High Calcium Fly Ash (HCFA). Compressive strength and electrical resistivity tests were used to evaluate the mortars' performance. A multi-regression (MR) model was also utilised to study the effects of curing time and content of OPC, GGBS and HCFA on the mortars' strength and to identify the relationship between measured and predicted compressive strengths. The results indicated that the newly developed binder was composed of 35 wt. % OPC, 35 wt. % GGBS and 30 wt. % HCFA that showed a compressive strength and surface electrical resistivity of 30.8 MPa and 103.5 kΩ.cm after 56 days of curing, respectively. Significant changes in the microstructure of the developed binder paste over curing time were evidenced by SEM imaging. The statistical analysis indicated that the influence of the parameters examined on the development of the mortars' compressive strength could be modelled with a coefficient of determination, R^2 of 0.893, and that the relative importance of these parameters followed the order curing time *(t)* > HCFA% > OPC% > GGBS%. This new binder could contribute significantly to decreasing the cost of construction materials and to reducing CO_2 emissions.

Keywords: Cementitious material; compressive strength; electrical resistivity, ground granulated blast furnace slag; high calcium fly ash; multiple regression.

1. Introduction

Greenhouse gases, global warming and waste management have become incredibly important issues worldwide. Universally, cement manufacturing creates approximately 7% of CO_2 emissions [1]. The production of one tonne of cement results in about one tonne of CO_2; it consumes approximately 5.6 GJ of energy and requires roughly 1.5 tonnes of raw materials to manufacture [2]. This ranks the cement industry as the third main producer of greenhouse gases, after transportation and energy generation sectors [3, 4]. In 2015, the world production of cement was around 4.6 billion tonnes. However, because of rapid development of the construction industry worldwide and an expected increase in the world population, it is estimated that the production of cement will reach around 9 billion tonnes by 2050 [5, 6].

The UK cement industry aims to reduce greenhouse gases, including CO_2, by around 81% relative to 1990 levels, by the end of 2050 [7, 8]. To achieve this, two methods are proposed, the first to reduce the production of cement. This however, cannot be achieved as the global population is increasing, creating a substantial expansion of infrastructure [9, 10]. The second, and more achievable method, is the replacement of cement with viable alternatives, where possible [11, 12].

Recently, significant interest has been shown in the production of blended cements incorporating Portland cement with supplementary cementitious materials (SCMs) from different resources. Research has been carried out with the aim of producing new (binary or ternary), environmentally friendly, cementitious materials with tailor-made properties [13-15]. Khalil and Anwar [13] reported that ternary blended cements could significantly enhance the performance of concrete compared with Ordinary Portland Cement (OPC) or binary blended cements. This is due to the blending operation where homogeneous nucleation may occur between various particle sized fractions leading to the development of a dense microstructure

of hardened product with higher durability [14]. Currently in several countries, there are numerous types of ternary blended cements with various combinations of OPC, with either ground granulated blast-furnace slag (GGBS) and fly ash, GGBS and silica fume (SF) or fly ash and SF which are more commonly used [13, 15].

There are still a number of obstacles that prevent ternary blended cements from being more universally applied such as the higher cost of SCMs (especially silica fume or metakaolin), the generation of larger amounts of heat during hydration, variability of the properties and the high water demand. This means that there is the need for various, cheap SCMs that could be used to produce low cost ternary blended cements with a comparable performance to conventional OPC or binary blended cements.

GGBS is one viable alternative SCM in the production of binary and ternary blended cements, and useful in different applications such as concrete production, soil stabilization and road construction [16-18]. GGBS, is a by-product of the iron industry and is extracted from blast furnaces [19]. Due to the chemical and physical properties of GGBS, it has many advantages relative to OPC, such as improved workability, enhanced durability and increased compressive strength [1, 20-22]. Because it is a very fine glassy powder, GGBS increases the bond between particles and minimises concrete permeability, thereby making the concrete more resistant to chloride ingress. This, in turn, protects the internal reinforcement from corrosion [23-25]. However, the presence of GGBS in high content could lead to increasing the depth of carbonation due to the reduced calcium hydroxide produced during hydration [26, 27].

Therefore, in order to produce a ternary blended cement with better performance than binary blending of GGBS-OPC cement, High Calcium Fly Ash (HCFA), a waste material that is produced from the burning process in local power plants, has been used in addition to OPC and GGBS.

HCFA is classified as fly ash class C. It has some self-cementing properties attributed to a high proportion of free lime, in addition to its pozzolanic properties [28, 29]. HCFA has been used by the authors in the production of binary and ternary blended binders as an alternative to cement in different applications [15, 30, 31].

Other new cementitious materials include those developed by Sadique et al. [15] using a high calcium fly ash (FA1), an alkali sulphate rich fly ash (FA2) and silica fume (SF), with a maximum of 5% waste gypsum incorporated as a grinding aid. The best mix to increase the compressive strength of mortars has been achieved using 60% FA1, 20% FA2 and 20% SF in addition to 5% waste gypsum as the grinding aid and a supplementary alkali activator e.g. NaOH. Jafer et al. [30] found that the ternary blending of HCFA, palm oil fuel ash (POFA) and rice husk ash (RHA) can be used as a cement replacement in the stabilisation of soft soil giving a superior performance to that of OPC. The efficacy of HCFA in road construction has been evidenced by Dulaimi et al. [31] who established that the combination of 4.5% HCFA with 1.5% fluid catalytic cracking catalyst (FC3R), improved the stiffness modulus by around 9% in comparison to a mixture treated with OPC alone.

Evaluating the durability performance of a new cementitious binder is essential factor when selecting a binder for mortar and concrete production. Recently, the use of electrical resistivity measurement techniques are becoming increasingly popular for the durability assessment of mortars and concrete [32-34]. Similar to the rapid chloride permeability test (RCPT), electrical resistivity can be used as a measure of mortar and concrete resistance to chloride penetration [34, 35]. Many studies have confirmed the suitability of the electrical resistivity measurement for assessing the chloride penetration of mortar and concrete as an alternative to the RCPT [34-36]. The test is non-destructive and can be performed faster and with less effort compared with RCPT while providing reliable results [35-37].

Researchers have shown a great deal of interest in the development of models to reproduce their experiments as they are of great benefit regarding the design process, optimisation and reproduction of experimental works [38, 39]. Therefore, part of the current study has been devoted to developing an empirical model to reproduce the development of the compressive strengths of mortars as a function of curing time (t) and the proportional contents of OPC, GGBS and HCFA in the newly developed binder.

In summary, this paper presents the results of the experimental work and statistical analysis modelling to study the influence of the partial replacement of OPC by GGBS and HCFA, using binary and ternary blending procedures, to produce a low carbon binder with properties comparable to OPC.

2. Materials and Methodology

2.1. Materials

2.1.1 Sand

The sand used in this investigation was 100% building sand passed through a 3.35mm IS sieve, with a specific gravity of 2.62 and a particle size distribution as shown in Fig 1.

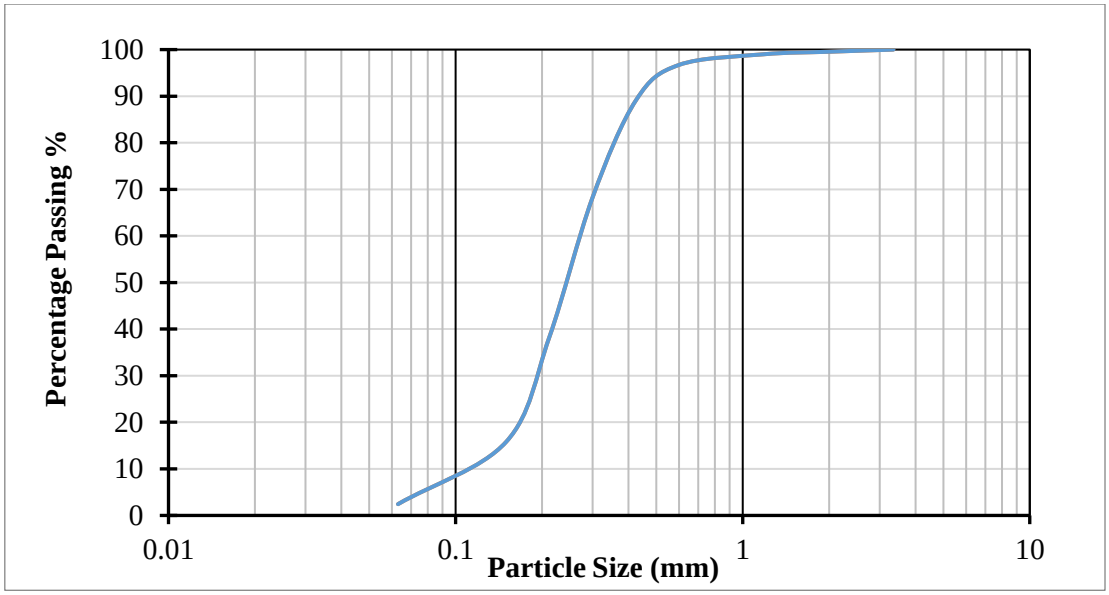

Fig. 1: Particle size distribution of the sand.

2.1.2 Water

Normal tap water supplied by United Utilities (city of Liverpool) was used in all mixtures.

2.1.3 Binder Materials

The materials used to produce the binders in this study were OPC, Ground Granulated Blast Furnace Slag (GGBS) and High Calcium Fly Ash (HCFA). The cement used in this study was OPC type CEM-II/A/LL 32.5-N. This cement was supplied by CEMEX Quality Department, Warwickshire, UK, and has a specific gravity of 2.936. The GGBS was provided by the Hanson Heidelberg Cement Group, Scunthorpe, UK, and has a specific gravity of 2.9. The HCFA is a waste material generated by power generation plants through combustion between 850^{o}C and 1100^{o}C, using a fluidised bed combustion system. It has a specific gravity of 2.78.

The PSD test was used to determine the fineness of the raw materials, utilising a Beckman Coulter laser particle size analyser. The specific surface area (SSA) of the raw materials was also measured using a Quantasorb NOVA 2000 Brunauer, Emmett and Teller (BET) analyser.

147 Fig. 2 shows the PSD curves for the OPC, GGBS and HCFA as obtained from the laser particle
148 size analyser. Table 1 shows the differences in d_{50} and the SSA of the raw materials.

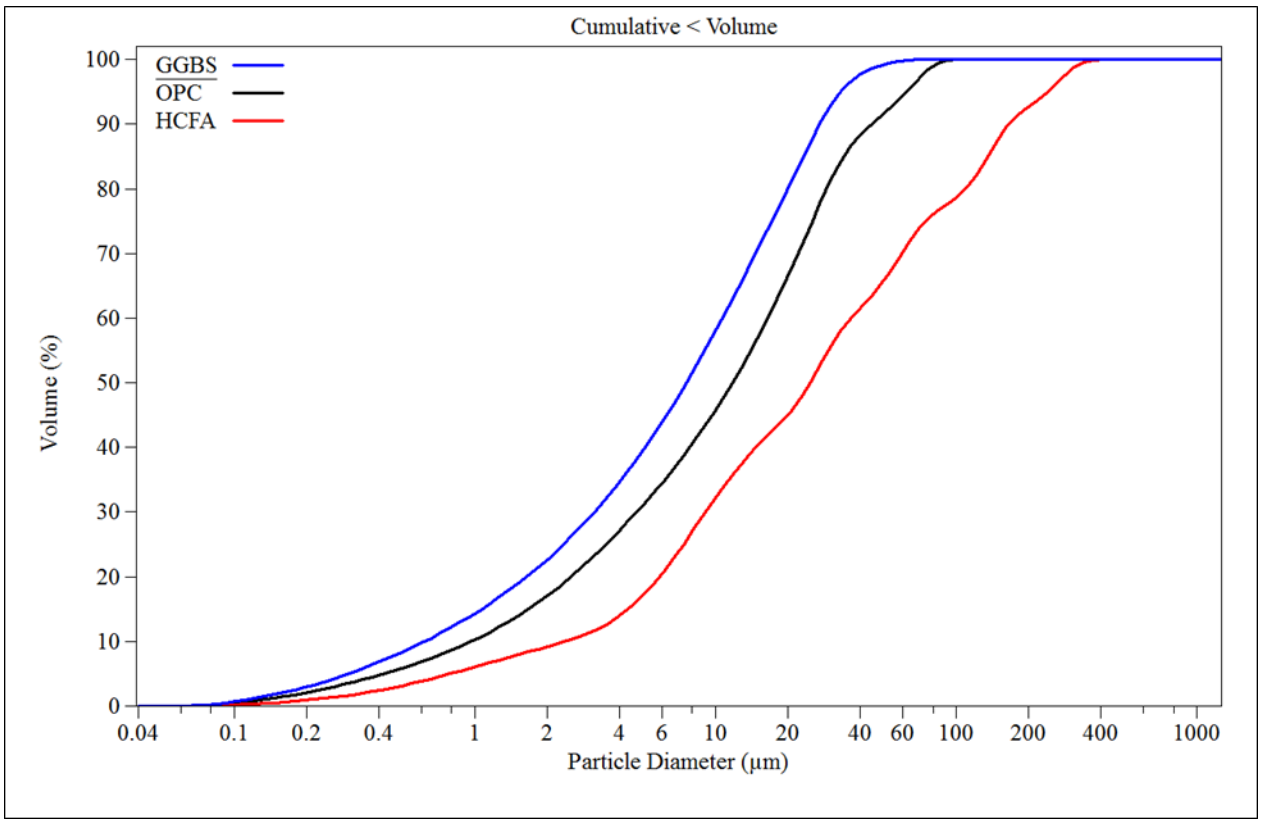

149

150 **Fig. 2:** Cumulative particle size distribution of OPC, GGBS and HCFA.

151

152 **Table 1:** The differences in d_{50} and the SSA of the raw materials.

Item	OPC	GGBS	HCFA
d_{50} (µm)	11.78	7.565	24.64
SSA (cm^2/mL)	29561	39671	16186

153

154 Both particle size distribution and the specific surface area of OPC, GGBS and HCFA, have a
155 significant effect on the compressive strength of the mortars. Celik et al. [40] found that the
156 finer the particles of waste materials used as partial replacement to cement in concrete

157 production, the higher the compressive strength obtained. It can be seen from the particle size
158 distribution charts in Fig. 2 that GGBS has finer particles relative to the other materials. In
159 contrast, HCFA has larger particles relative to OPC, which could retard the performance of
160 the mortars during hydration reactivity [30]. These results are in agreement with the findings
161 obtained by Jafer et al. [30] and Dulaimi et al. [31]

162 The elemental composition of OPC, GGBS and HCFA was analysed by an Energy Dispersive
163 X-ray Florescence Spectrometer (EDXRF) type Shimadzu EDX-720. This test identifies the
164 major oxide and trace elements in raw materials by breaking down the chemical composition.
165 Table 2 shows the chemical composition of the OPC, GGBS and HCFA.

166 From Table 2, it can be seen that the amount of CaO, SiO_2 and Al_2O_3 in the HCFA exceeds
167 that in the OPC. The chemical composition of the HCFA in this study are consistent with those
168 of Dulaimi et al. [41] and Jafer et al [30]. GGBS has significant proportions of most principle
169 oxides (CaO, SiO_2, MgO and Al_2O_3) and its (CaO+MgO)/SiO_2 is greater than 1.0, which meets
170 BS EN 197-1:2000 requirements for granulated blast furnace slag [42].

171 **Table 2:** Chemical composition of OPC, GGBS and HCFA.

Item	OPC	GGBS	HCFA
CaO %	65.21	42.51	66.67
SiO_2 %	24.56	41.06	25.12
Al_2O_3 %	1.70	5.12	2.38
Fe_2O_3 %	1.64	-	0.03
MgO %	1.30	4.25	2.57
Na_2O %	1.34	3.09	1.72
K_2O %	0.82	0.69	0.31
SO_3 %	2.62	1.27	0.26
TiO2 %	-	0.98	0.41
pH	12.73	11.02	12.82

172

2.2 Mixing Proportions

GGBS initially replaced OPC at various percentages: 10, 15, 20, 25, 30, 35, 40, 45 and 50% by mass of OPC, to create the optimum Binary Blended Cementitious Materials (BBCM). Following this, BBCM was partially replaced by HCFA in different percentages: 10, 15, 20, 25, 30, 35, 40, 45 and 50% by mass of BBCM to produce the new Ternary Blended Cementitious Material (TBCM). Tables 3 and 4 give the mixing proportions for the binary and ternary blending mixtures. The binder-to-sand ratio for all binary and ternary mixtures was fixed as 1:2.5, while the water to binder (W/B) ratios of the ternary mixtures were adjusted in order to achieve a good workability for each mixture [43].

Table 3: Mixing proportion for binary blending.

Mix ID	OPC (%)	GGBS (%)	W/B
R	100	0	0.4
OG10	90	10	0.4
OG15	85	15	0.4
OG20	80	20	0.4
OG25	75	25	0.4
OG30	70	30	0.4
OG35	65	35	0.4
OG40	60	40	0.4
OG45	55	45	0.4
OG50	50	50	0.4

Table 4: Mixing proportion for ternary blending.

Mix ID	BBCM (%)	HCFA (%)	W/B
T10	90	10	0.4
T15	85	15	0.4
T20	80	20	0.4
T25	75	25	0.45
T30	70	30	0.5
T35	65	35	0.55
T40	60	40	0.55
T45	55	45	0.55
T50	50	50	0.55

2.3 Testing Programme

2.3.1 Compressive strength

Compression testing was performed in accordance with BS EN 196-1 [44]. Samples of each of the binary and ternary mixtures were exposed to two different curing periods: 7 and 28 days, prior to the compression testing. Three samples of dimensions 40×40×160mm, were prepared for each mixing proportion and curing age. Each sample was broken into two halves by three point loading of the prism specimens and averages of six halves were taken to represent the final values for compressive strength. Additionally, the compressive strength test was conducted on the optimum TBCM at 3, 7, 28 and 56 days of curing and compared with that of the reference cement samples (R).

2.3.2 Electrical resistivity

The surface resistivity of mortar specimens was conducted for the evaluation the durability of the TBCM. This test was conducted using a Resipod Proceq surface resistivity meter that operates on the Wenner probe principle, whereby electrical resistivity is measured according to AASHTO T 358 [45]. This test is directly linked to the likelihood of corrosion due to chloride

220 diffusion [34, 37]. Three cylinders with a diameter of 100mm and a height of 200mm were
221 prepared and tested after 3, 7, 14, 21, 28 and 56 days for the TBCM and R samples. The
222 readings were obtained 8 times for each specimen and the averages of 24 readings were taken
223 to represent the final values for electrical resistivity to be used for comparison purposes. At the
224 time of testing, all the samples were in the condition of saturated surface dry in order to obtain
225 consistent measurements.

226 ***2.3.3 Standard consistency and setting time***

227 Standard consistency and setting time tests were conducted on the TBCM and R samplers using
228 the Vicat apparatus according to BS EN 196-3 [46].

229 ***2.3.4 Scanning Electron Microscopy (SEM)***

230 SEM testing was used to assess the morphology of each raw material in their powder states and
231 the TBCM paste, after 3, 28 and 56 days of curing. This testing was carried out using an EDX
232 Oxford Inca x-act detector, an FEI SEM model Inspect S and a Quanta 200 with an accelerating
233 voltage of 5-20 kV. Prior to SEM imaging, the samples were coated with a layer of gold using
234 a sputter coater for increased visibility.

235 ***2.4 Statistical Analysis and Modelling***

236 The data sets were statistically analysed to examine the relationships between the studied
237 parameters (curing time (*t)*, the percentage of OPC, GGBS, and HCFA) and mortar strength.
238 The influence of both curing time and the proportion of additive on the development of mortar
239 strength was modelled using a multiple regression (MR) technique. The latter was chosen
240 because of its ability to identify relationships among several variables [38]. The relative
241 importance of each individual parameters' contribution to mortar strength, was investigated by
242 determining the Beta coefficient (β) [47].

To develop a reliable MR model, the following assumptions must be examined: data set size, normality of data, presence of outliers and multicollinearity along with the normality, linearity and homoscedasticity (NLH) of residuals [47-49]. The ability of the developed model to explain the relationship between the independent and dependant parameters must be evaluated by calculating the coefficient of determination (R^2) [39].

Tabachnick and Fidell [50] recommended the following equation to calculate the minimum required data set size to develop a generalizable MR model:

$$data\ size > 50 + 8 \times number\ of\ independent\ variables \quad \textbf{(1)}$$

Normality of data can be checked using the Kolmogorov-Smirnov's test, the z-value of skewness (Z_s) and kurtosis (Z_k). The statistical significance (ρ) of the Kolmogorov-Smirnov test must be greater than 0.05, while the values of both Z_s and Z_k, (Eqs.2 and 3), must be within the range of ± 1.96 [51-54].

$$Z_k = \frac{K}{S_k} \quad \textbf{(2)}$$

$$Z_s = \frac{S}{S_s} \quad \textbf{(3)}$$

Where, K, S_k, S and S_s are the calculated kurtosis, the standard error for kurtosis, skewness and the standard error for skewness, respectively.

The existence of multicollinearity between independent variables, can be detected by calculating the tolerance value, where high tolerance values (> 0.1) indicate the absence of the multicollinearity [38]. The presence of outliers can be detected by calculating the standardised residuals (SR) for the data; any data point with an SR value out of the range 3.3 to -3.3, must be considered an outlier [50]. The Mahalanobis distance (MD) should be calculated for any outliers to see whether they need an additional analysis or not. Any outlier with an MD value

greater than the critical MD could have a negative influence on the outcome of the model [47]. In the current study, the critical MD value is 18.47 as four independent parameters have been investigated [48].

Finally, the NLH of residuals can be examined by creating a scatterplot of the standardised residuals (SR), where it is expected that less than 1% of the SR values of the data will exceed the range 3.0 to -3.0 [48].

In this study, the SPSS-24 package has been used to analyse the data and to develop the statistical model.

3. Results and Discussion

3.1 Compressive strength of mortars

3.1.1 Optimisation for binary blending

The compressive strengths of the mortars made from different combinations of OPC and GGBS at different curing ages, are shown in Fig. 3.

At 7 days of age, only OG10, OG20 and OG25 mixes provided better compressive strength than the control mix, R. However, at this age of curing, replacing OPC with 30% and 35% GGBS gave a slight reduction in the compressive strength of 3.6% and 5.1%, respectively. The substitution of OPC with 40, 45 and 50% GGBS, caused considerable reductions in the compressive strength in comparison to the control mix. This was due to the slow acquisition of strength at initial curing ages for the mixes containing 40% or higher GGBS [55, 56].

After 28 days of curing, the mixes which had GGBS added to them exhibited an enhanced compressive strength relative to the control mix, R. This means that it is necessary to extend the curing period of mixes with GGBS to ensure the development of compressive strength.

These results agree with the main findings of Mangamma et al. [57] and Cheng et al. [58]. As mix OG50 gained compressive strength, exceeding that for the control mix, at the same time reducing the amount of cement by 50%, it was judged the optimum binary mixture denoted as BBCM. The latter was used to produce the TBCM.

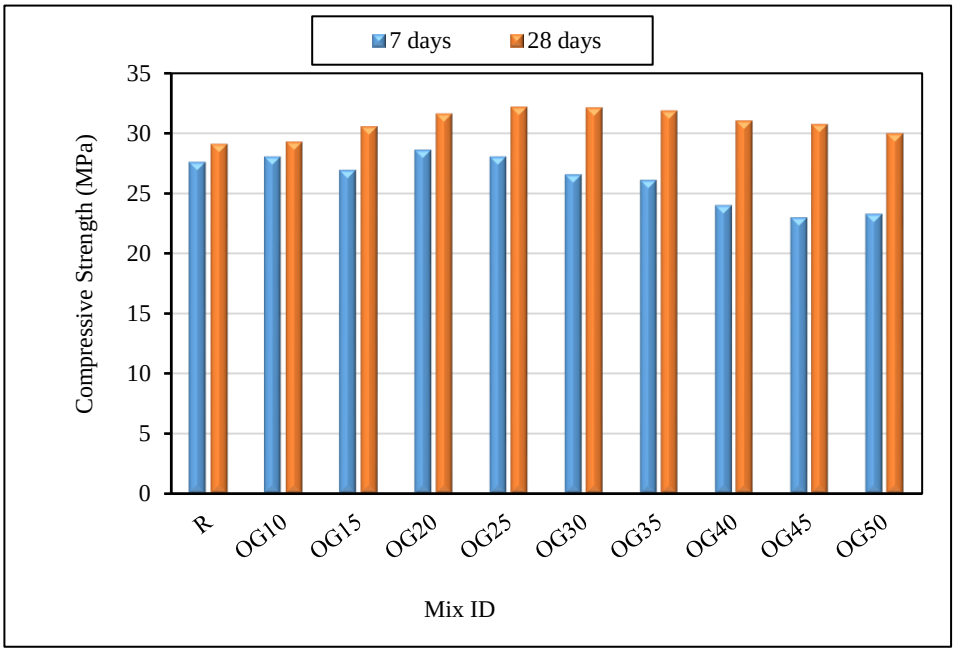

Fig. 3: Compressive strength development of different binary blends.

3.1.2 Optimisation for ternary blending

When mixing ternary blends, the most important thing to consider was how long the pozzolanic materials would take to react with calcium hydroxide to form hydration products [15]. The major advantage of developing a ternary blended product, relative to unary or binary mixtures, is an increase in particle packing leading to a denser microstructure that enhances the durability of the mortar [14]. In order to develop the TBCM, HCFA was added to the BBCM (OG50), in different percentages, as shown in Table 4. Fig. 4 shows the compressive strength of the mortars made from different combinations of BBCM and HCFA at different curing ages.

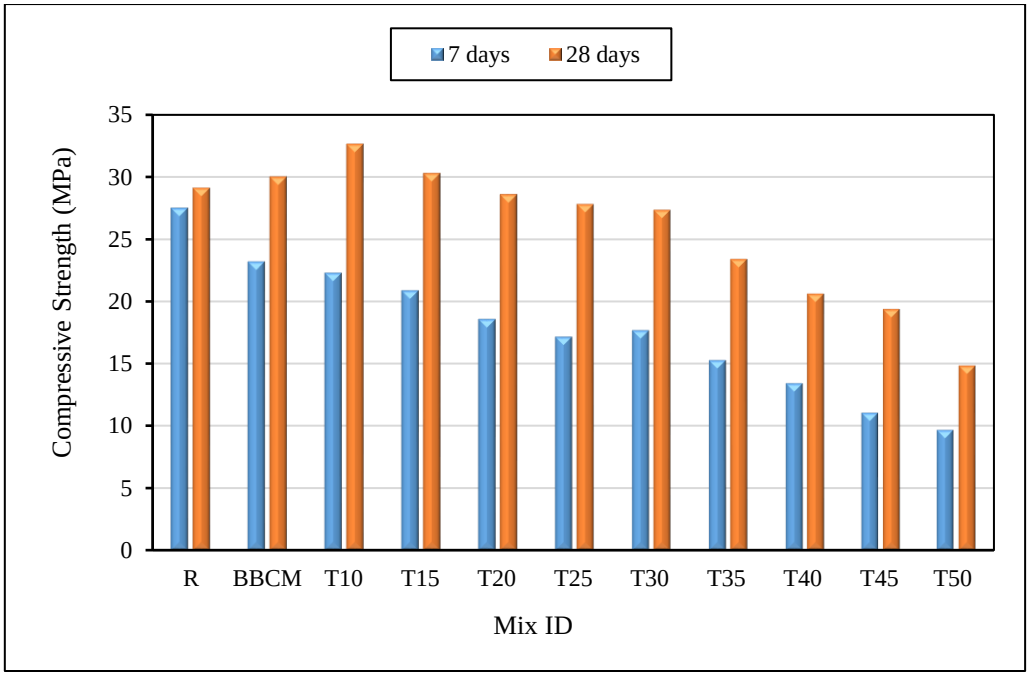

306

307 **Fig. 4:** Compressive strength development of different ternary blends.

308 It can be seen from Fig. 4 that at 7 days of age, all the ternary mixes have a lower compressive
309 strength than that of the control mix, R. This is because GGBS acquires strength slowly at the
310 initial stages of curing and because of the coarse HCFA particles, which can retard the
311 performance of the mortars during the hydration process [1, 16, 30]. The results of the
312 compressive strength tests after 28 days of curing indicated that the addition of 10% and 15%
313 of HCFA to BBCM improved the compressive strength by approximately 12% and 4%,
314 respectively, in comparison to the control mix, R. The mixes T20, T25 and T30 provided 98%,
315 96% and 94% of the compressive strength of the control mix, respectively.

316 In contrast, increasing the percentage of HCFA over 30% caused considerable reduction in the
317 compressive strength, ranging between 20% for T35 to approximately 50% for T50, relative to
318 the reference mix. This can be attributed to the increased water-to-binder ratio that was required
319 to improve workability; increasing the percentage of HCFA increases the water demand in the
320 mixes [59]. The increase of water demand would also contribute to cause the reduction in

compressive strength because this increasing in water will be associated with more porosity due to the greater spacing between binder particles [60].

In conclusion, the T30 with 30% HCFA was chosen as the newly developed TBCM to be used for subsequent compressive strength, electrical resistivity, standard consistency, setting time and SEM investigation.

3.2 Statistical Analysis and Modelling

According to Eq. 1, the minimum amount of data required to perform the MR is 82 data points. This requirement was met as the collected data set consists of 132 data points.

The results obtained from the Kolmogorov-Smirnov test indicated that the data does not follow a normal distribution because its ρ value (0.01) is less than the threshold value of 0.05, which is not favourable for MR. Therefore, the data has been mathematically normalised using the natural logarithm function. The ρ value, after normalization, increased to 0.200. Both the Z_s and Z_k values then fell within the range 0.207 to -1.623 that are within the recommended range (± 1.96) [51-54], which in turn confirms the normality of the data.

The existence of multicollinearity between independent variables was investigated by calculating the tolerance values for the studied parameters. The results indicated an absence of multicollinearity as the values of tolerance were greater than 0.1 (Table 5).

However, Table 5 shows that there are two outliers within the data (their SR exceeded the range of 3.3 to -3.3); these could significantly influence the outcomes of the model. Therefore, the MD of these two outliers was calculated to check whether or not they exert a significant influence on the outcomes of the model. These values were below the threshold value of 18.47 indicating that these two outliers do not exert a significant influence on the predictability of the proposed MR model. It is noteworthy to highlight that the threshold value is calculated

according to the number of the studied parameters [48]. In the current study, the threshold value is 18.47 as four independent parameters have been investigated [48]. Although it has been confirmed that these two outliers do not exert a significant influence on the outcomes of the developed model, they could influence other statistical parameters such as the mean and standard deviation [48]. Therefore, these two data points were removed before testing the last assumption to avoid any minor negative influence.

Finally, the NLH of residuals were investigated by checking the standardised residuals (SR) of the studied data, where it is expected that less than 1% of the SR values of the data will exceed the range 3.0 to -3.0. Table 5 shows that all the SR values of the data were within the permissible range (3.0 to -3.0).

Table 5: Summary of statistical analysis results.

Parameter	Tolerance	Sig.	Presence of outliers (SR exceeded the range of 3.3 to -3.3)		MD	NLH (SR exceeded the range of 3.0 to -3.0)	
			No. of cases	SR value		No. of cases	SR value
t	0.991	0.000					
$OPC\%$	0.52	0.048	65	3.341	4.64	None	None
$GGBS\%$	0.111	0.050	70	-3.670	5.25		
$HCFA\%$	0.89	0.000					

Based on the results obtained from the statistical analyses, the influence of the studied parameters ($t, OPC\%, GGBS\%, and\ HCFA\%$) on the development of the strength of the mortars can be represented by Equation 4:

$$Strength\ (MPa) = \omega\ (5.426 + 0.041\ t - 0.008\ OPC\% - 0.005\ GGBS\% - 0.04\ HCFA\%)^2 + \gamma e^{(1.33+0.28t+0.001OPC\%-0.001GGBS\%-0.015HCFA\%)} \quad \textbf{(4)}$$

Where, $\omega\ and\ \gamma$ are the model combination factors, with values given in Equations 5 and 6:

$$\omega = \begin{cases} 1 \; when \; t \; > 7 \; days \\ \\ 0.0 \; when \; t \; \leq 7 \; days \end{cases} \quad \textbf{(5)}$$

$$\gamma = \begin{cases} 0.0 \; when \; t \; > 7 \; days \\ \\ 1 \; when \; t \; \leq 7 \; days \end{cases} \quad \textbf{(6)}$$

To evaluate how strongly each parameter influences the outcomes of the MR model, the β value was calculated for each individual parameter. Fig. 5 shows that the relative importance of the studied parameters followed the order: $curing\ time\ (t) >$ HCFA% > OPC% > GGBS%.

Before applying the proposed model to a random dataset, the ability of the developed model to explain the relationship between mortar strength and the studied parameters must be evaluated. The calculated R^2 value, (0.893), confirms the ability of the suggested model to explain 89.3% of the variance in mortar strength.

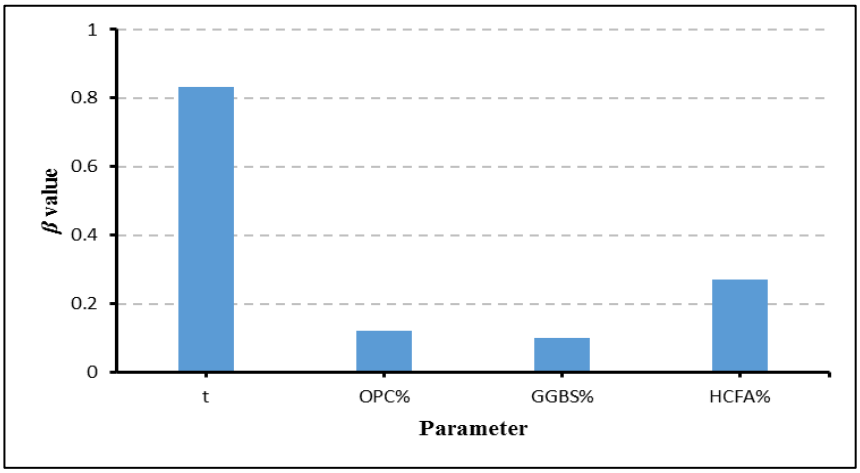

Fig. 5. Contribution of each parameter to the outcomes of the proposed model.

To investigate the level of agreement between the predicted and measured mortar strengths, the model was applied to a randomly selected set of experimental data consisting of 46 data points. To avoid any statistical bias, these random points were selected using SPSS-24 software. Fig. 6 reveals a good level of agreement between the predicted and experimental readings, the R^2 value for this random dataset being 0.8731.

The results of statistical analyses indicate that the MR model is able to reproduce the development of mortar strength within the range of parameters included in this study.

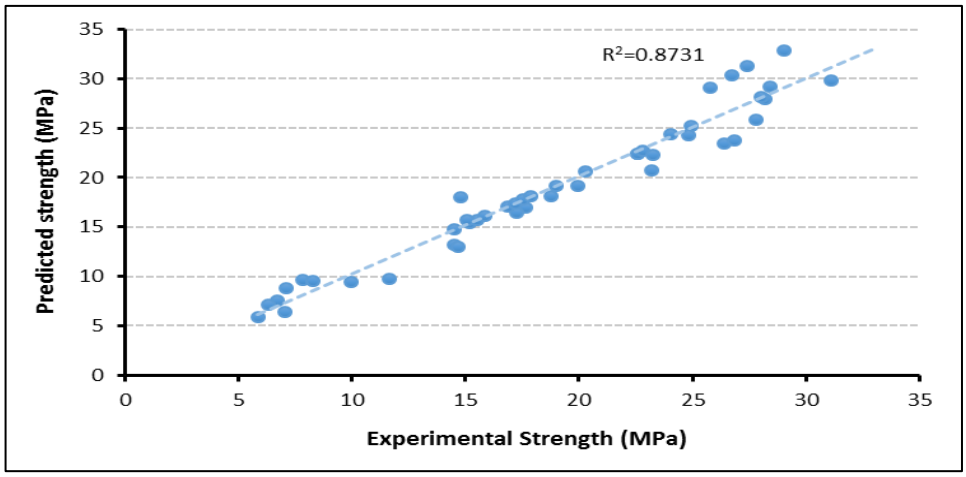

Fig. 6. Predicted vs Experimental mortar strength for the randomly selected dataset.

3.3 Comparative study of the TBCM and the reference cement (R)

3.3.1 Compressive strength

The comparative compressive strength development of the TBCM and R has also been displayed in Fig. 7. This revels that the strength development of TBCM at early ages (3 and 7 days) was slower than that of R. This is because SCMs acquire strength slowly at the initial stages of curing. At later curing ages (28 and 56 days), the strength development of TBCM was very similar to the reference cement.

The successful improvements in strength after 7 days of curing is attributed to the formation of additional C-S-H gel from both the chemical reaction occurring between the lime from the HCFA and amorphous silica provided by GGBS together with the high alkalinity environment of HCFA, which enhanced the dissolution of the glassy phases of GGBS producing additional C-S-H gel [14, 61, 62]. This leads to a successful hydration reaction, transforming the calcium hydroxide of HCFA into calcium silicate hydrate (C-S-H) [15, 61]. This gel tends to fill pores and grow into capillary spaces, resulting in a more impermeable, dense and higher-strength structure [61-63].

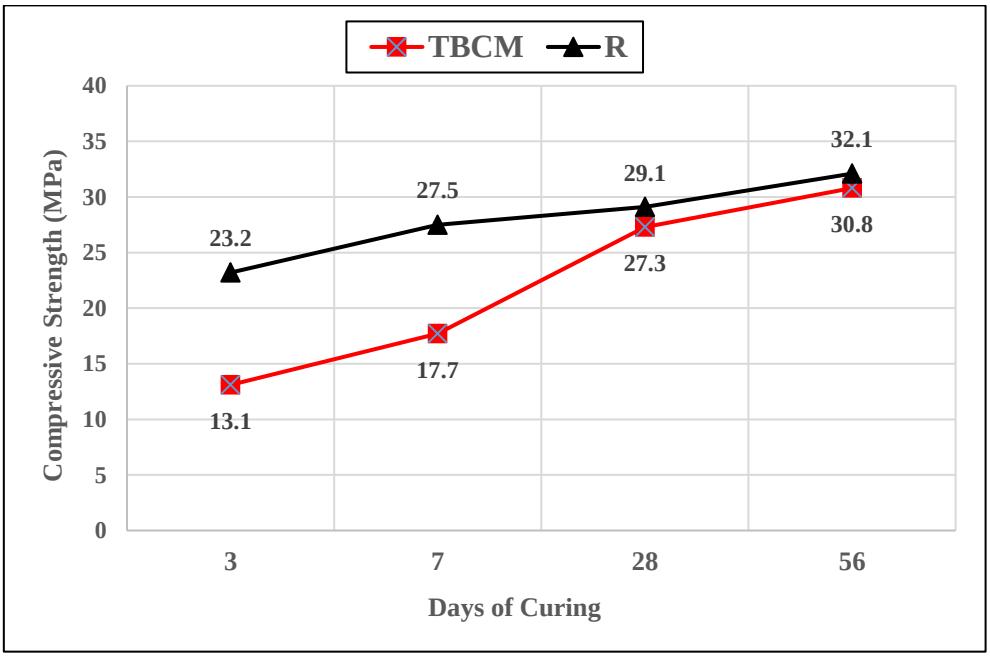

Fig. 7. Comparative strength development of TBCM and reference cement mortar.

The newly developed TBCM had comparable compressive strength to that of the control mix, R, at the same time reducing the amount of cement used in the total binder by 65%. Such a replacement will contribute significantly to reductions in CO_2 emissions, reducing the overall cost of construction and providing comparable performance in an adequate curing time.

3.3.2 Electrical Resistivity

The results of the electrical resistivity testing for the TBCM and R samples at 3, 7, 14, 21, 28 and 56 days are presented in Fig. 8.

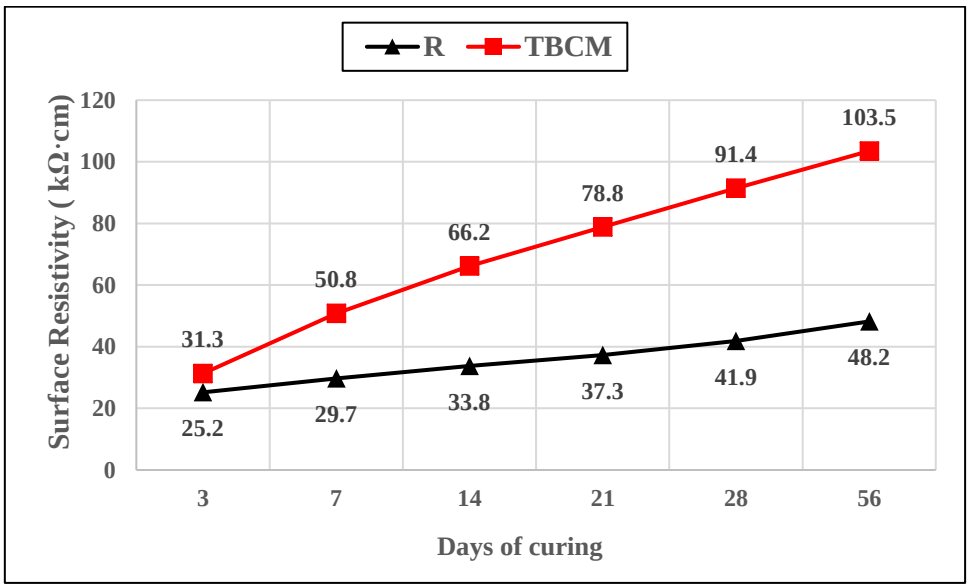

Fig. 8. Comparative electrical resistivity development of TBCM and reference cement mortar.

It can be seen from Fig. 8 that the surface electrical resistivity of the TBCM and R samples was enhanced with increasing age of curing. Fig.8 also indicates a clear improvement in the surface resistivity of TBCM relative to R at all curing ages. This improvement in surface resistivity means that TBCM is more resistant to chloride penetration in comparison with R [33-35, 37]. The enhanced resistance of TBCM to chloride penetration is mainly attributed to the incorporation of GGBS and HCFA that leads to reduced diffusivity of chloride ions due to higher packing density and increased C-S-H gel, thus leading to a denser microstructure in the developed ternary blend [1, 14, 25, 34].

In order to better evaluate the chloride resistance of TBCM and to compare it with that of the reference cement, the results of the electrical resistivity were compared with a chloride penetration classification as published by the AASHTO T 358 [45]. Based on AASHTO T 358 classification, both TBCM and R at 3 days have shown a low chloride ion penetrability. At the

age of 7 days of curing onward, the TBCM has produced a very low chloride ion penetrability. Regarding the reference cement, the results indicated that it has a low chloride ion penetrability until the age of 21 days then after that moved to very low chloride ion penetrability. In summary, such findings demonstrated that the incorporation of GGBS and HCFA as partial replacement to OPC in the TBCM have significantly enhanced the durability properties of mortar relative to conventional OPC for the scope of this investigation.

3.3.3 Standard Consistency and Setting Time

The standard consistency and setting time tests were conducted for the newly developed TBCM and compared with that of R. The consistency test depends mainly on the water to binder ratio, fineness and rate of hydration reactions of the binder [64]. The results of the standard consistency of the TBCM and R mixes are shown in Table 6. The results indicate that the incorporation of GGBS and HCFA increased the water demand of the mixes. This could be attributed to both the higher specific surface area of GGBS relative to OPC and the high void spaces that illustrated the high porosity and high water demand of HCFA as can be seen from the SEM image of the HCFA in Fig 9 [15, 64]. Segui et al. [65] reported that the increase in water demand of binder materials with an agglomerated morphology is due to the increase in the water absorbed by the large open areas of high porosity. This is in agreement with the results of standard consistency carried out by Sadique, et al., [14] who found that the consistency of a new ternary blend cementitious binder containing 60% HCFA was 68%, which was around 2.5 times the consistency of OPC mix.

Regarding the initial and final setting times, this test was conducted after determining the standard consistency of TBCM and R. The results of initial and final setting times of TBCM and R are shown in Table 6. The results of setting time indicated a significant reduction in both initial and final setting times of the TBCM relative to R. This reduction could be mainly due

444 to the higher specific surface area of GGBS in comparison to OPC and the presence of highly
445 reactive phases represented by the high CaO content as a major component of the HCFA, which
446 accelerates the hydration reaction [66, 67]. Previously, Sadique, et al. [14] demonstrated that
447 using fly ash with a high CaO content reduced the setting time of the mix relative to OPC.

448 **Table 6**. Standard consistency and setting time results

Test	**R**	**TBCM**
Standard Consistency	33%	50%
Initial Setting Time (min)	265	80
Final Setting Time (min)	285	95

449

450 ***3.3 SEM observations***

451 SEM is a method of scanning that provides detailed, high-resolution images of sample surfaces
452 [47]. SEM is the most widely used technique, in the cement research sector, for the morphology
453 analysis of hardened products and the evaluation of the degree of hydration [15, 45]. Although
454 SEM is a surface sensitive technique, it can still provide plentiful information about the surface
455 reactions of the sample [68]. This is of particular interest as the surface of the sample is the
456 first place that any reactions will occur [64, 65]. The SEM tests were conducted on each raw
457 material to identify the general shape of particles, thus aiding to elucidate the performance of
458 these materials when they were combined to produce binary or ternary mixtures [45].

459 The SEM images for the raw materials shown in Fig. 9 indicate that both OPC and GGBS
460 particles have an irregular shapes and that OPC particles are coarser than those of GGBS, this
461 being in agreement with the results of the PSD tests. The HCFA particles are agglomerated

and have a coagulated state occurring in clusters. This is in agreement with the findings obtained by Jafer et al [36] and Dulaimi et al [48].

.

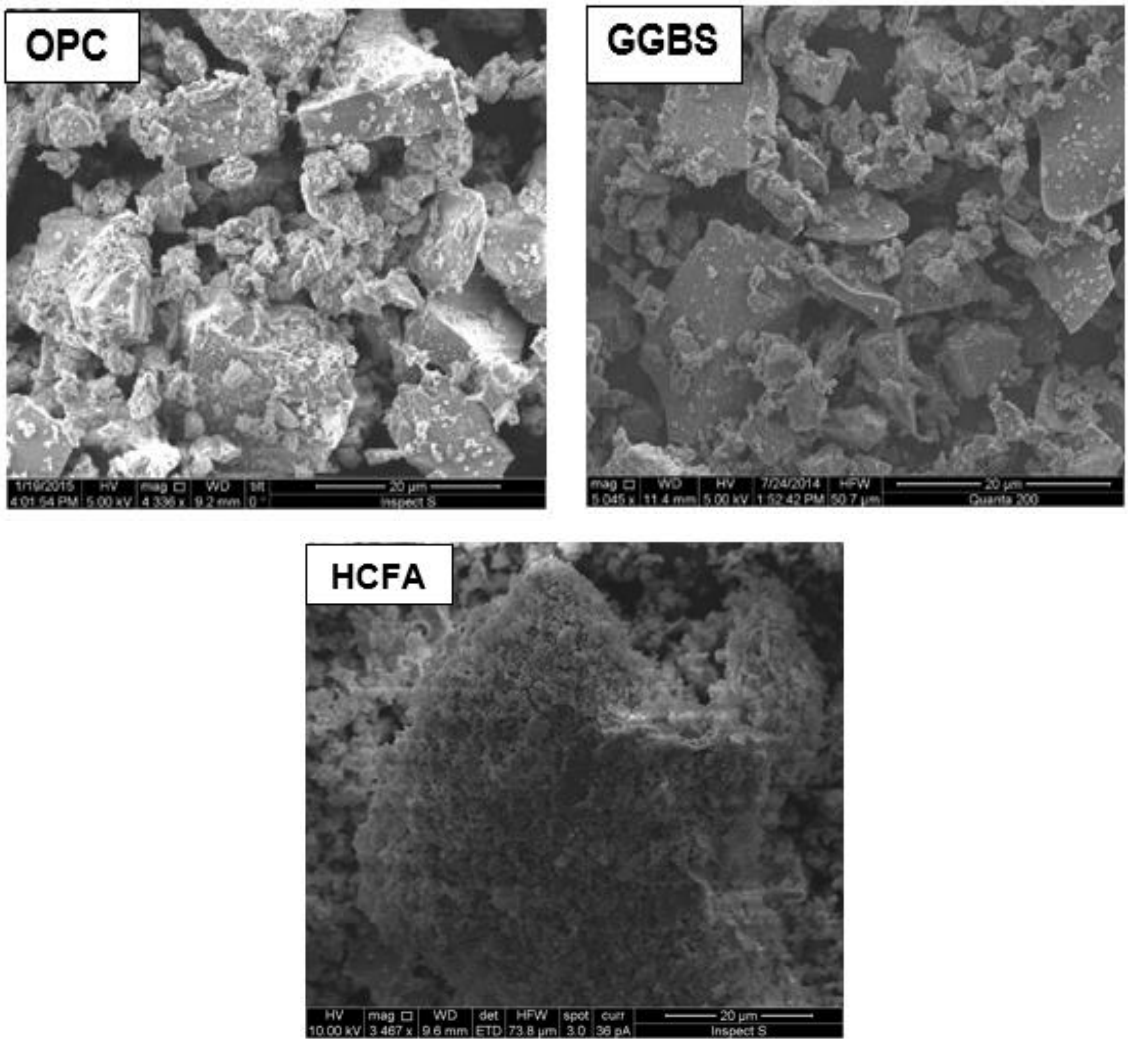

Fig. 9. SEM images of the raw materials (dry powder)

The SEM micrographs of the fractural surface of the TBCM paste after 3, 28 and 56 days, are presented in Fig. 10. This figure clearly evidenced the formation of needle-like ettringite, a consequence of initial hydration [15, 69], the formation of flaky shaped crystals (Portlandite (CH)) and C-S-H gel, the main strength-generating material responsible for providing the binding and strengthening properties of the mix [14] at 3 days of curing.

At all the curing ages, no intact powder particles of raw materials were detected; the OPC, GGBS and HCFA particles were transformed into hydration products due to a successful

hydration reaction (Fig. 10). The 28 days SEM images indicated a denser microstructure for the TBCM paste with less ettringite and CH crystals detected. At the age of 56 days, a very dense microstructure of TBCM was observed, where the surface of the TBCM paste is almost completely covered by C-S-H gel.

As time passed, it was found that most of the pore voids were filled with C-S-H gel, resulting in a compact and dense microstructure, significantly enhancing the strength and durability of the newly developed cementitious binder. These observations were consistent with the development gained in the compressive strength and electrical resistivity of the TBCM. Similar findings were reported by Jafer et al. [30], Sadique et al. [14], and Scrivener et al. [68].

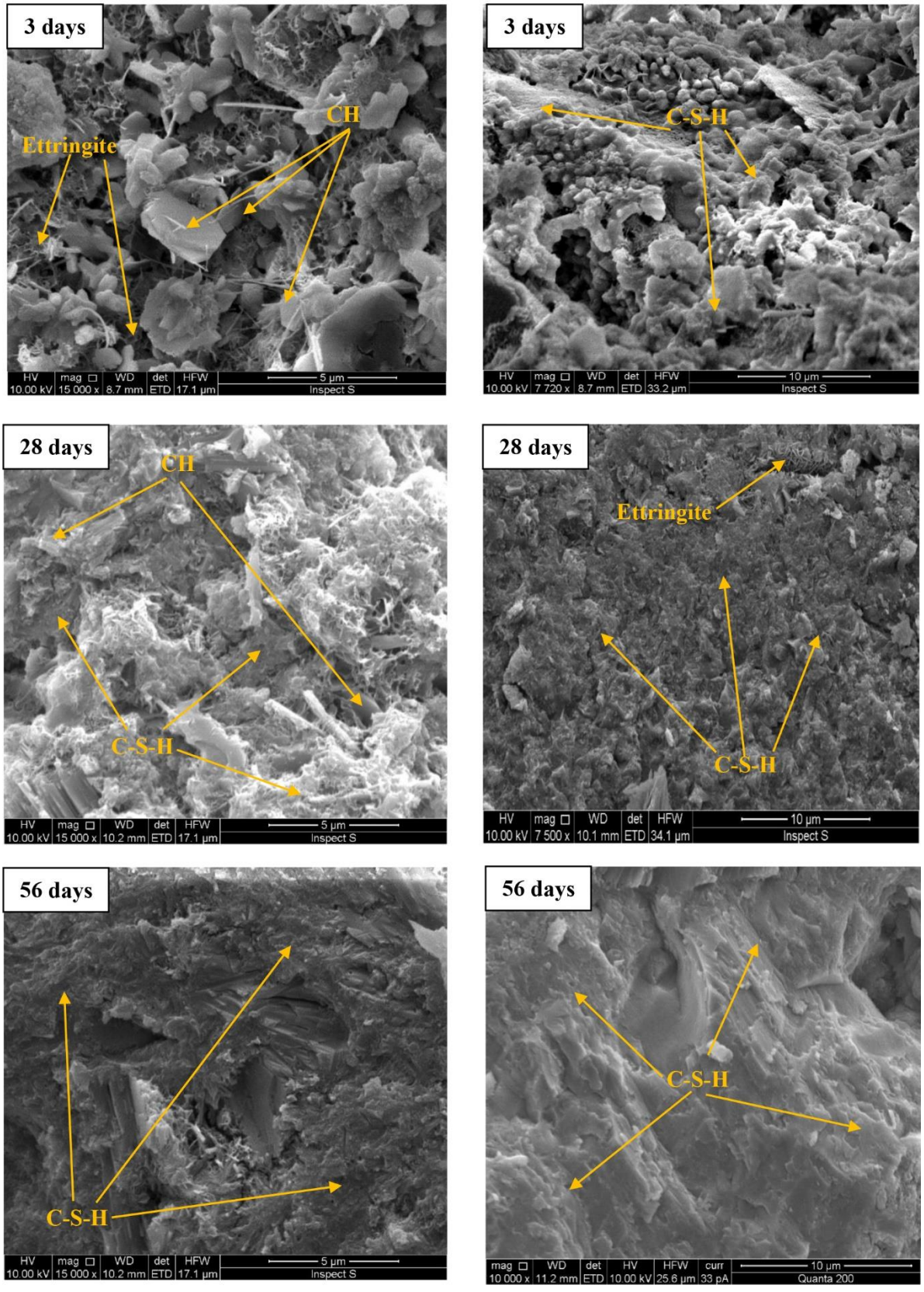

Fig. 10. The micrographs of the TBCM paste at 3, 28 and 56 days of curing. (Left column 5 μm and right column 10 μm ranges).

4. Conclusion

The aim of this study was to develop a new cementitious material by blending OPC with different proportions of GGBS and HCFA, to produce an environmentally friendly cementitious material. Based on the results of the experimental work and statistical modelling, the following conclusions have been drawn:

- A new, ternary blended cementitious material (TBCM) was developed from (35% OPC + 35% GGBS + 30% HCFA). This binder can be used for commercial cement replacement in mortar, concrete production and soft soil stabilisation or as a filler for road construction. Reducing the OPC content in the total binder by 65% could contribute to the reduction of the negative environmental footprint created by the manufacture of cement.
- The compressive strength of the new TBCM mortar has been found to increase from 13.1MPa after 3 days to 30.8MPa after 56 days. The 56 days compressive strength value of the TBCM represents about 96% of the compressive strength of mortars made with reference cement (32.1MPa).
- Regarding the durability aspects, the results indicated an enhanced electrical resistivity of the TBCM relative to the reference cement, R at all curing ages. In addition, after 7 days of curing, the TBCM has shown a very low chloride ion penetrability.
- In terms of consistency and setting time, the water demand of the TBCM was higher than that of the OPC by 17%. In addition, both initial and final setting time of the TBCM paste were significantly decreased relative to that of pure cement paste.
- The characteristics of the new TBCM, as identified by the SEM tests, confirmed the results of the compressive strength and durability tests, providing evidence for the suitability of the new product to be used in different applications in place of OPC.

- The results of the statistical analyses indicated that the MR model was able to reproduce the development of mortar strength within the range of parameters included in this study. The relative importance of these parameters follows the order: curing time (t) > HCFA% > OPC% > GGBS%.
- As the performance of the developed binder depends to large extent on the properties of the investigated SCMs (GGBS and HCFA), therefore the replacement of any of them with other SCMs means that the optimized levels and performance will not be the same as those of the developed binder.

Acknowledgments

The first author would like to acknowledge the financial support provided for this research by Mr. Abdulhussein Shubbar, together with Babylon and Kerbala Universities, Iraq. The authors would also like to thank the Hanson Heidelberg Cement Group for the free cost of supply of GGBS for this research. This research was carried out in the concrete laboratory at Liverpool John Moores University.

References

[1] Hawileh, R.A., J.A. Abdalla, F. Fardmanesh, P. Shahsana, and A. Khalili, *Performance of reinforced concrete beams cast with different percentages of GGBS replacement to cement.* Archives of Civil and Mechanical Engineering, 2017. **17**(3): p. 511-519.

[2] O'Rourke, B., C. McNally, and M.G. Richardson, *Development of calcium sulfate–ggbs–Portland cement binders.* Construction and Building Materials, 2009. **23**(1): p. 340-346.

[3] Bains, P., P. Psarras, and J. Wilcox, *CO 2 capture from the industry sector.* Progress in Energy and Combustion Science, 2017. **63**: p. 146-172.

[4] The Guardian. *Which industries and activities emit the most carbon?* 2011 [cited 2017 7/11]; Available from: https://www.theguardian.com/environment/2011/apr/28/industries-sectors-carbon-emissions.

[5] Aprianti S, E., *A huge number of artificial waste material can be supplementary cementitious material (SCM) for concrete production – a review part II.* Journal of Cleaner Production, 2017. **142**: p. 4178-4194.

[6] Department of Energy & Climate Change, *2013 UK Greenhouse Gas Emissions, Final Figures*, in *Statistical release*. 2015, National Statistics.

[7] Wang, J.-W., H. Liao, B.-J. Tang, R.-Y. Ke, and Y.-M. Wei, *Is the CO 2 emissions reduction from scale change, structural change or technology change? Evidence from non-metallic sector of 11 major economies in 1995–2009.* Journal of Cleaner Production, 2017. **148**: p. 148-157.

[8] MPA Cement, *The UK cement industry aims to reduce greenhouse gases by 81% by 2050*. 2013: London.

[9] Yang, K.-H., J.-K. Song, and K.-I. Song, *Assessment of CO2 reduction of alkali-activated concrete.* Journal of Cleaner Production, 2013. **39**: p. 265-272.

[10] Aprianti, E., P. Shafigh, S. Bahri, and J.N. Farahani, *Supplementary cementitious materials origin from agricultural wastes – A review.* Construction and Building Materials, 2015. **74**: p. 176-187.

[11] Habert, G., J.B. d'Espinose de Lacaillerie, and N. Roussel, *An environmental evaluation of geopolymer based concrete production: reviewing current research trends.* Journal of Cleaner Production, 2011. **19**(11): p. 1229-1238.

[12] McLellan, B.C., R.P. Williams, J. Lay, A. van Riessen, and G.D. Corder, *Costs and carbon emissions for geopolymer pastes in comparison to ordinary portland cement.* Journal of Cleaner Production, 2011. **19**(9-10): p. 1080-1090.

[13] Khalil, E.A.B. and M. Anwar, *Carbonation of ternary cementitious concrete systems containing fly ash and silica fume.* Water Science, 2015. **29**(1): p. 36-44.

[14] Sadique, M., H. Al Nageim, W. Atherton, L. Seton, and N. Dempster, *A new composite cementitious material for construction.* Construction and Building Materials, 2012. **35**: p. 846-855.

[15] Sadique, M., H. Al-Nageim, W. Atherton, L. Seton, and N. Dempster, *Mechano-chemical activation of high-Ca fly ash by cement free blending and gypsum aided grinding.* Construction and Building Materials, 2013. **43**: p. 480-489.

[16] Gholampour, A. and T. Ozbakkaloglu, *Performance of sustainable concretes containing very high volume Class-F fly ash and ground granulated blast furnace slag.* Journal of Cleaner Production, 2017. **162**: p. 1407-1417.

[17] Nassar, A.I., M.K. Mohammed, N. Thom, and T. Parry, *Mechanical, durability and microstructure properties of Cold Asphalt Emulsion Mixtures with different types of filler.* Construction and Building Materials, 2016. **114**: p. 352-363.

[18] Sharma, A.K. and P.V. Sivapullaiah, *Ground granulated blast furnace slag amended fly ash as an expansive soil stabilizer.* Soils and Foundations, 2016. **56**(2): p. 205-212.

[19] Grist, E.R., K.A. Paine, A. Heath, J. Norman, and H. Pinder, *The environmental credentials of hydraulic lime-pozzolan concretes.* Journal of Cleaner Production, 2015. **93**: p. 26-37.

[20] Jianyong, L. and Y. Yan, *A study on creep and drying shrinkage of high performance concrete.* Cement and Concrete Research, 2001. **31**: p. 1203 - 1206.

[21] Khan, K.M. and U. Ghani. *Effect of blending of portland cement with ground granulated blast furnace slag on the properties of concrete* in *29th Conference on OUR WORLD IN CONCRETE & STRUCTURES*. 2004. Singapore.

[22] Sangeetha, S.P. and P.S. Joanna, *Flexural Behaviour of Reinforced Concrete Beams with Partial Replacement of GGBS.* American Journal of Engineering Research (AJER), 2014. **3**(1): p. 119-127.

[23] Barnett, S.J., M.N. Soutsos, S.G. Millard, and J.H. Bungey, *Strength development of mortars containing ground granulated blast-furnace slag: Effect of curing temperature and determination of apparent activation energies.* Cement and Concrete Research, 2006. **36**(3): p. 434-440.

[24] Dinakar, P., K.P. Sethy, and U.C. Sahoo, *Design of self-compacting concrete with ground granulated blast furnace slag.* Materials & Design, 2013. **43**: p. 161-169.

[25] Islam, A., U.J. Alengaram, M.Z. Jumaat, and I.I. Bashar, *The development of compressive strength of ground granulated blast furnace slag-palm oil fuel ash-fly ash based geopolymer mortar.* Materials & Design (1980-2015), 2014. **56**: p. 833-841.

[26] Lye, C.-Q., R.K. Dhir, and G.S. Ghataora, *Carbonation resistance of GGBS concrete.* Magazine of Concrete Research, 2016. **68**(18): p. 936-969.

[27] McNally, C. and E. Sheils, *Probability-based assessment of the durability characteristics of concretes manufactured using CEM II and GGBS binders.* Construction and Building Materials, 2012. **30**: p. 22-29.

[28] Ghosh, A. and C. Subbarao, *Strength Characteristics of Class F Fly Ash Modified with Lime and Gypsum.* Journal Of Geotechnical And Geoenvironmental Engineering, 2007. **133**(7): p. 757-766.

[29] Jafer, H.M., W. Atherton, F. Ruddock, and E. Loffill. *The Stabilization of a Soft Soil Subgrade Layer Using a New Sustainable Binder Produced from Free-Cement Blending of Waste Materials Fly Ashes*. in *10th international conference on the bearing capacity of roads, railways and airfields*. 2017. Athens, Greece.

[30] Jafer, H.M., W. Atherton, M. Sadique, F. Ruddock, and E. Loffill, *Development of a new ternary blended cementitious binder produced from waste materials for use in soft soil stabilisation.* Journal of Cleaner Production, 2018. **172**: p. 516-528.

[31] Dulaimi, A., H. Al Nageim, F. Ruddock, and L. Seton, *New developments with cold asphalt concrete binder course mixtures containing binary blended cementitious filler (BBCF).* Construction and Building Materials, 2016. **124**: p. 414-423.

[32] Afroughsabet, V. and T. Ozbakkaloglu, *Mechanical and durability properties of high-strength concrete containing steel and polypropylene fibers.* Construction and Building Materials, 2015. **94**: p. 73-82.

[33] Sengul, O., *Use of electrical resistivity as an indicator for durability.* Construction and Building Materials, 2014. **73**: p. 434-441.

[34] Zahedi, M., A.A. Ramezanianpour, and A.M. Ramezanianpour, *Evaluation of the mechanical properties and durability of cement mortars containing nanosilica and rice husk ash under chloride ion penetration.* Construction and Building Materials, 2015. **78**: p. 354-361.

[35] Layssi, H., P. Ghods, A. Aali R. , and M. Salehi, *Electrical Resistivity of Concrete, Concepts, applications, and measurement techniques*. 2015, Concrete International.

[36] Sengul, O. and O.E. Gjørv, *Electrical resistivity measurements for quality control during concrete construction.* ACI Materials Journal, 2008. **105**(6): p. 541-547.

[37] Turner-Fairbank Highway Research Centre, *Surface Resistivity Test Evaluation as an Indicator of the Chloride Permeability of Concrete*. 2012: McLean, Virginia, United States.

[38] Hashim, K.S., A. Shaw, R. Al Khaddar, M. Ortoneda Pedrola, and D. Phipps, *Defluoridation of drinking water using a new flow column-electrocoagulation reactor (FCER) - Experimental, statistical, and economic approach.* Journal of Environmental Management, 2017. **197**: p. 80-88.

[39] Jafer, H.M., K.S. Hashim, W. Atherton, and A.W. Alattabi, *A Statistical Model for the Geotechnical Parameters of Cement-Stabilised Hightown's Soft Soil: A Case Study of Liverpool, UK.* International Journal of Civil, Environmental, Structural, Construction and Architectural Engineering, 2016. **10**(7): p. 885 - 890.

[40] Celik, O., E. Damci, and S. Paskin, *Characterisation of fly ash and its effect on the compressive strength properties of portland cement.* Indian Journal of Engineering & Materials Science 2008. **15**(5): p. 433-440.

[41] Dulaimi, A., H.A. Nageim, F. Ruddock, and L. Seton, *Performance Analysis of a Cold Asphalt Concrete Binder Course Containing High-Calcium Fly Ash Utilizing Waste Material.* Journal of Materials in Civil Engineering, 2017. **29**(7): p. 04017048.

[42] European Committee for Standarization, *Cement - Part 1: Composition, specifications and conformity criteria for common cements*. 2000, British Standard Institution: London.

[43] Chindaprasirt, P., S. Homwuttiwong, and C. Jaturapitakkul, *Strength and water permeability of concrete containing palm oil fuel ash and rice husk–bark ash.* Construction and Building Materials, 2007. **21**(7): p. 1492-1499.

[44] BSI, *Methods of testing cement–Part 1: Determination of strength*. 2005, British Standard Inistitute: London.

[45] AASHTO T 358, *Standard Method of Test for Surface Resistivity Indication of Concrete's Ability to Resist Chloride Ion Penetration*. 2017, American Association of State and Highway Transportation Officials.: Washington DC.

[46] British Standard Institution, *Method of testing cement. Determination of setting time and soundness, BS EN 196-3 and A1*. 2008, British Standard Institution.: London

[47] Hashim, K.S., A. Shaw, R. Al Khaddar, M.O. Pedrola, and D. Phipps, *Iron removal, energy consumption and operating cost of electrocoagulation of drinking water using a new flow column reactor*. Journal of Environmental Management, 2017. **189**: p. 98-108.

[48] Pallant, J., *SPSS SURVIVAL MANUAL*. 2nd ed. 2005, Australia: Allen & Unwin. 318.

[49] Hashim, K.S., A. Shaw, R. Al Khaddar, M.O. Pedrola, and D. Phipps, *Energy efficient electrocoagulation using a new flow column reactor to remove nitrate from drinking water - Experimental, statistical, and economic approach.* J Environ Manage, 2017. **196**: p. 224-233.

[50] Tabachnick, B.G. and L.S. Fidell, *Using Multivariate Statistics*. 5th ed. 2001, Boston: Allyn and Bacon.

[51] Heffron, J., *Removal of Trace Heavy Metals from Drinking Water by Electrocoagulation*, in *The faculty of the Graduate School*. 2015, Marquette University.

[52] Musheer, Z., P. Govil, and S. Gupta, *Attitude of Secondary Level Students towards Their School Climate.* Journal of Education and Practice, 2016. **7**(19): p. 39-45.

[53] Sleight, V.A., A. Bakir, R.C. Thompson, and T.B. Henry, *Assessment of microplastic-sorbed contaminant bioavailability through analysis of biomarker gene expression in larval zebrafish.* Mar Pollut Bull, 2017. **116**(1-2): p. 291-297.

[54] Shiota, S., Y. Okamoto, G. Okada, K. Takagaki, M. Takamura, A. Mori, S. Yokoyama, Y. Nishiyama, R. Jinnin, R.I. Hashimoto, and S. Yamawaki, *Effects of behavioural activation on the neural basis of other perspective self-referential processing in subthreshold depression: a functional magnetic resonance imaging study.* Psychol Med, 2017. **47**(5): p. 877-888.

[55] Attari, A., C. McNally, and M.G. Richardson, *A probabilistic assessment of the influence of age factor on the service life of concretes with limestone cement/GGBS binders.* Construction and Building Materials, 2016. **111**: p. 488-494.

[56] Limbachiya, V., E. Ganjian, and P. Claisse, *Strength, durability and leaching properties of concrete paving blocks incorporating GGBS and SF*. Construction and Building Materials, 2016. **113**: p. 273-279.

[57] Mangamma, B., N. Victor babu, and G. Hymavathi, *An Experimental Study on Behavior of Partial Replacement of Cement with Ground Granulated Blast Furnace Slag.* Int. Journal of Engineering Research and Application, 2016. **6**(12): p. 1 - 4.

[58] Cheng, A., R. Huang, J.-K. Wu, and C.-H. Chen, *Influence of GGBS on durability and corrosion behavior of reinforced concrete.* Materials Chemistry and Physics, 2005. **93**(2-3): p. 404-411.

[59] Tangchirapat, W. and C. Jaturapitakkul, *Strength, drying shrinkage, and water permeability of concrete incorporating ground palm oil fuel ash.* Cement and Concrete Composites, 2010. **32**(10): p. 767-774.

[60] Aïtcin, P.C., *The importance of the water–cement and water–binder ratios*, in *Science and Technology of Concrete Admixtures*. 2016. p. 3-13.

[61] Jafer, H., W. Atherton, M. Sadique, F. Ruddock, and E. Loffill, *Stabilisation of soft soil using binary blending of high calcium fly ash and palm oil fuel ash.* Applied Clay Science, 2018. **152**: p. 323-332.

[62] Wild, S., J.M. Kinuthia, G.I. Jones, and D.D. Higgins, *Effects of partial substitution of lime with ground granulated blast furnace slag (GGBS) on the strength properties of lime-stabilised sulphate-bearing clay soils.* Engineering Geology, 1998. **51**: p. 37-53.

[63] Blanco, F., M.P. Garcia, J. Ayala, G. Mayoral, and M.A. Garcia, *The effect of mechanically and chemically activated fly ashes on mortar properties.* Fuel, 2006. **85**(14-15): p. 2018-2026.

[64] Dave, N., Misra, A. K., Srivastava, A. & Kaushik, S. K.,, *Experimental analysis of strength and durability properties of quaternary cement binder and mortar*. Construction and Building Materials, 2016. **107**: p. 117-124.

[65] Segui, P., J.E. Aubert, B. Husson, and M. Measson, *Characterization of wastepaper sludge ash for its valorization as a component of hydraulic binders.* Applied Clay Science, 2012. **57**: p. 79-85.

[66] Lee, N.L., H., , *Setting and mechanical properties of alkali-activated fly ash/slag concrete manufactured at room temperature*. Construction and Building Materials 2013. **47**: p. 1201-1209.

[67] Salih, M.A., N. Farzadnia, A.A. Abang Ali, and R. Demirboga, *Development of high strength alkali activated binder using palm oil fuel ash and GGBS at ambient temperature.* Construction and Building Materials, 2015. **93**: p. 289-300.

[68] Scrivener, K., A. Bazzoni, B. Mota, and J.E. Rossen, *A Practical Guide to Microstructural Analysis of Cementitious Materials*, ed. K. Scrivener, R. Snellings, and B. Lothenbach. 2016, Boca Raton, Florida, United States. : CRC Press.

[69] Dodds, L., *Microstructure Characterisation of Ordinary Portland Cement Composites for the Immobilisation of Nuclear Waste*, in *Faculty of Engineering and Physical Sciences*. 2012, University of Manchester: UK.